NEURONAL NETWORK STRUCTURAL CONNECTIVITY ESTIMATION BY PROBABILISTIC FEATURES AND GRAPH HEAT KERNELS

S. Ullo[1]*, U. Castellani*[2]*, D. Sona*[1]*, A. Del Bue*[1]*, A. Maccione*[3]*, L. Berdondini*[3]*, V. Murino*[1]

[1] Pattern Analysis and Computer Vision (PAVIS)
Istituto Italiano di Tecnologia
Genova, Italy

[2] Dept. of Computer Science
University of Verona
Verona, Italy

[3] Neuroscience and Brain Technologies (NBT)
Istituto Italiano di Tecnologia
Genova, Italy

ABSTRACT

It is well proven that the functional electrophysiological behavior of *in-vitro* neuronal networks is influenced by the structural connectivity. Thus, the automatic extraction of the topology in large assemblies of interconnected neurons can be a valuable tool for investigating the basic mechanisms underlying high-level cognitive functions. In this paper we propose a method for estimating the structural connectivity of neuronal networks from multimodal datasets combining high-resolution Multi-Electrode Arrays (MEA) and fluorescence microscopy. Probabilistic directional features are used in a graph heat kernel framework to identify the structural connectivity of the neuronal network. Electrode connectivity maps are computed as weighted graphs in which the edge weights represent the strength of the structural connection.

Index Terms— Structural Connectivity, Graph Heat Kernel, Von Mises Density, Neuronal Networks, Multi-Electrode Array

1. INTRODUCTION

Dissociated neuronal cultures, even if randomly connected, show electrical activity patterns that are involved in the basic mechanisms underlying high-level cognitive functions. These functional properties result from the cooperative interaction of single neurons, showing how the structural connectivity can profoundly impact the electrophysiological activity [1]. This highlights the importance of understanding how neurons are topologically interconnected in complex networks.

The Multi-Electrode Array technology (MEA) [2, 3], allows for single-cell monitoring of the electrical activity of sparse *in-vitro* neuronal networks by recording the neuronal electrophysiological signal. In combination, high-resolution fluorescence microscopy allows for the acquisition of the corresponding network morphology, depicting both neuronal nuclei and arborizations. This results in highly complex datasets offering a quasi one-to-one mapping between recording electrodes and interconnected neurons. Such multimodal datasets require advanced computational approaches for inferring structural and functional connectivity patterns. However, current methods for the analysis of high-resolution MEA datasets mainly involve techniques based on signal correlation used to infer functional connections between electrodes [4]. In these methods, the structural information coming from the fluorescence microscopy image is often discarded because of the high network complexity which makes any manual assessment unfeasible. This yields to an increasing need for automated methods capable of inferring the structural connectivity in large images with thousands of interconnected neurons.

Despite the high image resolution of current microscopy technologies, neuronal arborizations usually appear very confused, presenting intricate crossing branches which are often very difficult to characterize, even for a human observer (see Fig. 4). Traditional methods found in the literature [5, 6] usually address the segmentation of single neuron's dendrites, axons and synapses (neuronal tracing [7]) from microscopy images, or are limited to very small assemblies where only the connectivity with a neuron's immediate neighbors is examined. In order to identify more complex behavioral patterns and infer information at network-level processing, a broader network connectivity analysis is required, which still represents a very challenging and quite unexplored task.

In this paper we address this task by proposing a novel method for inferring the structural connectivity in neuronal networks using high-resolution MEA and fluorescence microscopy multimodal datasets. In this setting, the structural connectivity of the network can be described as a graph, where nodes correspond to electrodes and edges represent morphological connections, weighted by a strength factor. The ultimate goal is providing a description of the network topology in terms of electrode connectivity, which represents a crucial step in relating the structural organization to the functional signal. Indeed, as the MEA-recorded electrophysiological signal is electrode-oriented, representing the morphology as a graph on electrodes can facilitate a joint analysis of structural and functional connectivity patterns. The proposed approach extracts maps of electrode connectivity using a graph heat kernel method [8, 9] based on probabilistic directional features. Specifically, the approach aims at finding the topological connectivity of a neuronal network by estimating a weighted graph representing the structurally interconnected electrodes and the strength of each connection. The method

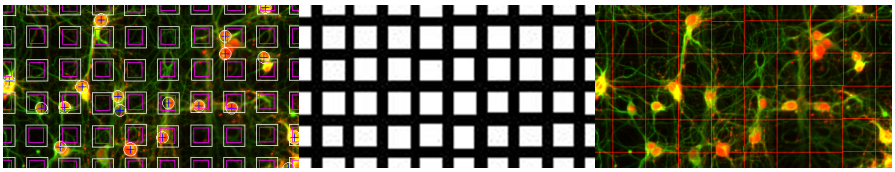

(a) (b) (c)

Fig. 1: Partition of the fluorescence image. (a) Results of the nuclei detection and electrode array reconstruction obtained as described in [3]. Circles and crosses show the neuronal nuclei, white and magenta squares are the reconstructed electrodes. (b) The binary mask for the electrode grid. (c) The final partition obtained by Watershed Transform.

exploits the regular MEA layout to partition the fluorescence image into patches and extract probabilistic features based on Mixtures of Von Mises distributions describing the underlying arbor architecture. The obtained features are then used in a graph heat kernel framework to obtain connectivity maps, as described in Section 2.2.

The remainder of the paper is organized as follows. A detailed description of the proposed method is provided in Section 2. Section 3 shows the experimental results. Finally, conclusions and future work are outlined in Section 4.

2. PROPOSED METHOD

As the high-density MEA technology provides a single-cell resolution, a direct mapping between neurons and electrodes can be extracted from the fluorescence image [3]. This is done by first locating the neuronal nuclei and reconstructing the electrode array partially visible on the image background, i.e. determining the location of each electrode (Fig. 1a). The recovered electrode grid is then used to partition the image into a lattice from which the probabilistic features will be extracted. In particular, electrode location and size are used to compute a binary mask of the electrode grid (Fig. 1b). The Watershed Transform [10] is then applied to obtain a partition of the image into a number of small patches, each corresponding to a single electrode area (Fig. 1c). We assume the patch size being small enough to describe the underlying arborizations by a combination of line segments.

Afterwards, a probabilistic directional feature is extracted at each image patch, locally representing the neuronal arbor architecture. As this information directly affects the degree at which electrodes are structurally interconnected, such local features are then used to define a global weighted adjacency matrix expressing the probability of two adjacent electrodes being structurally connected (see Section 2.2). Finally, the obtained adjacency matrix is used within a graph heat kernel framework to compute an electrode connectivity map.

2.1. Probabilistic Directional Feature

We want the local directional feature to characterize the predominant arbor orientations in a probabilistic fashion, i.e. providing, for each electrode, the probability of connection in every possible neighboring direction. Such a probabilistic feature is obtained by firstly approximating the underlying network structure as a set of n_i line segments, extracted at the i-th image patch by using a gradient-based Hough Transform (HT). Thus, the i-th patch will be assigned the set of segments s_k:

$$S_i = \{s_k(\Psi, A, B, \nu)\}_{k=1,2,\ldots,n_i}, \quad (1)$$

where $\Psi = (\rho, \theta)$ are the support line parameters in the Hough space, A and B are the two segment endpoints and ν is the Hough vote. Hough votes are globally normalized to make them comparable among different patches. Based on set S_i, a Von Mises Mixture (VMM) model is defined for each patch, in order to obtain a probabilistic representation of local arbor architecture. Von Mises distributions are particularly suitable for directional statistics, representing a probability density defined on the circumference [11]. The generic Von Mises distribution is defined as:

$$\mathcal{V}(\theta; \mu, \kappa) = \frac{e^{\kappa \cos(\theta-\mu)}}{2\pi I_0(\kappa)}, 0 \leq \theta < \pi, \quad (2)$$

where μ is the mean, κ is the concentration and I_0 is the modified Bessel function of the first kind of order 0. The VMM model is formulated by the mixture:

$$\text{VMM}(\theta) = \sum_{i=1}^{M} w_i \mathcal{V}_i(\theta), \quad (3)$$

with w_i being the mixture proportions, such that $0 \leq w_i \leq 1$ and $\sum_{i=1}^{M} w_i = 1$.

In our case, the VMM construction can be described as follows. Given a segment $s \in S_i$ with endpoints A and B, we consider its support line intersecting the patch boundary at two points, named A' and B'. We denote with $d_{AA'}$ and $d_{BB'}$, respectively, the euclidean distances between the two pairs of points (A, A') and (B, B') (see Fig. 2). Since the segment s can be considered as the evidence of a real structural

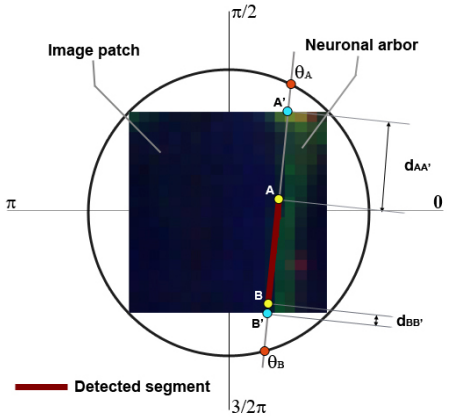

Fig. 2: Construction of the Von Mises Mixture (VMM) model. Model parameters are determined on the basis of the line segments detected by the Hough Transform.

connection in the image, the two distances $d_{AA'}$ and $d_{BB'}$ can be interpreted as a measure of the uncertainty in determining the orientation of the arbor defined by s. In other words, the bigger the distance $d_{AA'}$ ($d_{BB'}$), the higher the uncertainty of the arbor crossing the patch boundary *exactly* at point A' (B'), i.e. having an arbor orientation defined by the angle θ_A (θ_B). Therefore, the orientation of a segment can be probabilistically modeled as a mixture of the two following Von Mises distributions:

$$\mathcal{V}_A(\theta; \mu_A = \theta_A, \kappa_A \propto d_{AA'}) \quad (4)$$

$$\mathcal{V}_B(\theta; \mu_B = \theta_B, \kappa_B \propto d_{BB'}) \quad (5)$$

with mixture proportions $\pi_A = \pi_B = \widetilde{\nu}/2$, where $\widetilde{\nu}$ is the normalized Hough vote. Hence, for a patch with n segments, the VMM will consist of $2n$ components, as shown in Fig. 3.

Once the VMM model has been defined, the last step in constructing the probabilistic directional feature consists in discretizing the probability density of the mixture so as to obtain a measure of connectivity among adjacent patches. This discretization process computes the area under the p.d.f. in each of the 8 circumference sectors corresponding to the 8 neighboring directions and results in a histogram H indicating the probability of each patch (electrode) being connected with its neighbors, according to a 8-neighborhood system (Fig. 3).

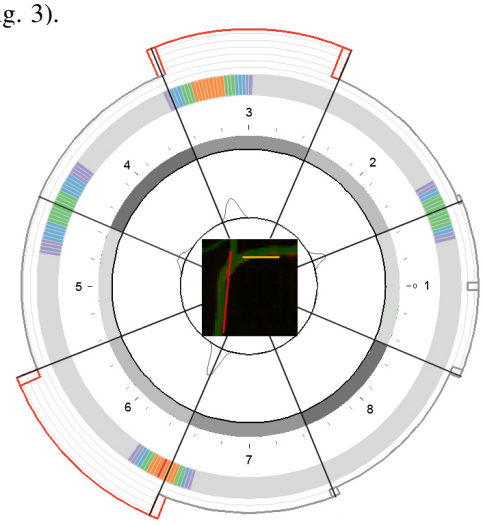

Fig. 3: Probabilistic directional feature representation. The segments detected by the HT are used to build the VMM model shown in the inner circle. The second circle shows the circumference sectors for the feature discretization (in different gray levels, numbered from 1 to 8). The third circle shows a heatmap for the pointwise p.d.f. values. Finally, the outer circle shows the histogram feature describing the probability of connection in each of the 8 neighboring directions.

2.2. Graph Heat Kernel

Given a graph $G = (V, E)$, where V is the set of nodes and $E \subseteq V \times V$ is the set of edges, the heat diffusion on G is defined by the *heat* equation [9, 8]:

$$\left(L_G + \frac{\partial}{\partial t}\right) u(t, x) = 0; \quad (6)$$

where $u(t, x)$ is the heat distribution at time t and L_G is the *Graph Laplacian* operator [12]. In particular $L_G = D - A$, where A is the *adjacency matrix* defined on graph G [12], and D is the *diagonal degree* matrix whose diagonal elements are given by $D(i, i) = \sum_{j \in V} A(i, j)$. According to spectral graph theory [9], the *heat kernel* has the following eigendecomposition [8]:

$$k_t(x, y) = \sum_{i=0}^{\infty} e^{-\lambda_i t} \phi_i(x) \phi_i(y), \quad (7)$$

where λ_i and ϕ_i are the i^{th} eigenvalue and eigenvector of the Graph Laplacian, respectively.
The heat kernel $k_t(x, y)$ is the solution of the heat equation with point heat source at x at time $t = 0$, i.e. the heat value at point y after time t [9]. In particular, the heat kernel encodes information about the distribution of path lenghts and therefore node affinities on the graph which, in our work, is defined on the grid of electrodes. The output of the heat kernel is a matrix indicating the electrode connectivity in terms of amount of heat propagated after time t and is normalized to obtain the final connectivity map.

In our work, the weighted adjacency matrix A is obtained from the probabilistic directional feature, by defining each element $A(i, j)$ as the histogram value for the edge connecting electrode i to electrode j. In other words, given an electrode i, we consider the histogram H_i extracted at the corresponding patch and set the 8 entries of matrix A matching its neighbors as the probabilities of connection defined by the histogram. Since the feature extraction process generally results in non-symmetric histogram values among neighboring electrodes, the matrix A is symmetrized by computing $A' = (A^T + A)/2$, i.e. by averaging the histogram values in the two edge directions.

It is worth noting that in the heat kernel computation the time parameter t plays a crucial role. Short-time periods keep the heat close to the starting node, while conversely longer periods let the heat exploring a larger portion of the graph.

3. RESULTS

The proposed method was evaluated against ground truth (GT) data, as shown in Fig. 4. Due to the subjectivity and error-proneness of ground truth acquisitions, five experts were asked to annotate 10 different datasets by indicating pairs of structurally connected electrodes. A final estimate of the ground truth was then obtained by adopting a voting strategy. From the analysis of the acquired GT it was possible to assess an average agreement between experts of 85%.

The best value for the time parameter t of the heat kernel framework was estimated on different runs of the algorithm by computing the Precision-Recall performance at times $t = 1, 2, 3, 5, 10, 20, 50$ (Fig. 5). At low t values the heat propagates for a shorter time interval, hence the algorithm cannot explore the whole space of connections. This results in a higher number of false negatives (lower recall) because some longer-distance structural connections are not detected. On the other hand, with a high t value false positives increase

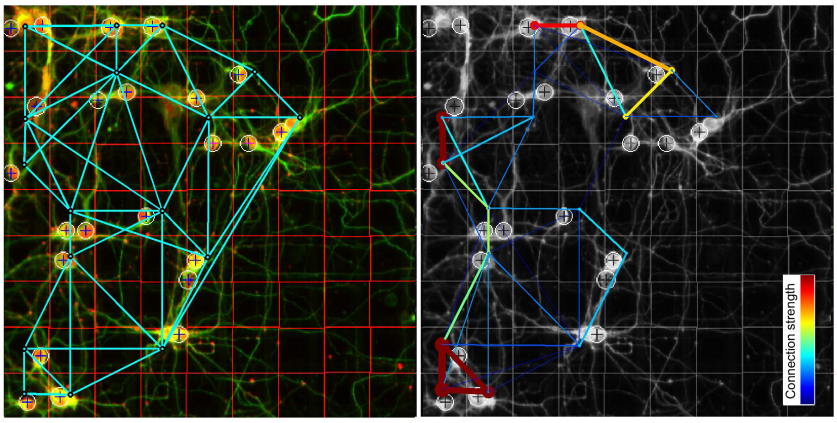

(a) (b)

Fig. 4: An example of connectivity graphs obtained with the proposed method (best viewed in color). (a) The ground truth showing structurally connected electrodes with straight lines (cyan). (b) The weighted graph obtained at $t = 10$. Electrode connections are color-coded with a heat colormap and their widths are proportional to the link strength.

and the precision drops off. In our case, the value of parameter t basically reflects the number of steps performed by the algorithm for exploring the discretized electrode-based feature space, where the graph is defined on a regular grid. From our experiments, in datasets with a 9×9 electrode array, a time interval equal to 10 or 20 suffices to successfully explore the whole space, obtaining the best F1-score.

Table 1 shows the algorithm performance for each dataset and the average Precision-Recall obtained at $t = 10$.

Dataset	Precision	Recall
1	71%	83%
2	59%	84%
3	39%	81%
4	89%	48%
5	86%	86%
6	72%	68%
7	50%	74%
8	75%	75%
9	75%	54%
10	61%	76%
Mean	**68%**	**73%**

Table 1: Performance of the proposed method for the 10 datasets at $t = 10$.

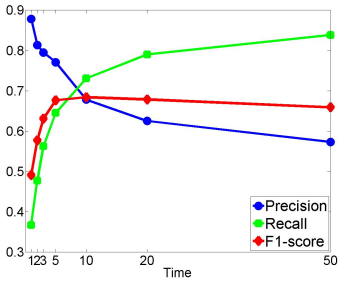

Fig. 5: Precision-Recall and F1-score performances at varying Time parameter.

4. CONCLUSIONS

In this paper we have presented a new method for the automatic estimation of the structural connectivity in multimodal datasets of *in-vitro* neuronal networks. The proposed approach takes advantage of a graph heat kernel framework based on probabilistic directional features to provide a weighted graph of connectivity defined on the electrode grid. Results show that, despite of the high dataset complexity, the algorithm performs quite well, also considering the average experts' agreement on the GT data.

Future work will address a joint analysis of the extracted structural information and the electrophysiological signal in order to infer relationships between structural and functional connectivity in neuronal networks.

5. REFERENCES

[1] B.C. Wheeler and G.J. Brewer, "Designing neural networks in culture," *Proceedings of the IEEE*, vol. 98, no. 3, pp. 398 –406, march 2010.

[2] L. Berdondini, K. Imfeld, A. Maccione, M. Tedesco, S. Neukom, M. Koudelka-Hep, and S. Martinoia, "Active pixel sensor array for high spatio-temporal resolution electrophysiological recordings from single cell to large scale neuronal networks.," *Lab on a Chip*, vol. 9, no. 18, pp. 2644–2651, 2009.

[3] S. Ullo, A. Del Bue, A. Maccione, L. Berdondini, and V. Murino, "A joint structural and functional analysis of in-vitro neuronal networks," 2012, IEEE International Conference on Image Processing.

[4] A. Maccione, M. Garofalo, T. Nieus, M. Tedesco, L. Berdondini, and S. Martinoia, "Multiscale functional connectivity estimation on low-density neuronal cultures recorded by high-density cmos micro electrode arrays," *Journal of Neuroscience Methods*, vol. 207, no. 2, pp. 161 – 171, 2012.

[5] J. Xie, T. Zhao, T. Lee, E. Myers, and H. Peng, "Automatic neuron tracing in volumetric microscopy images with anisotropic path searching.," *International Conference on Medical Image Computing and Computer-Assisted Intervention (MICCAI)*, vol. 13, no. Pt 2, pp. 472–9, Jan. 2010.

[6] P. Chothani, V. Mehta, and A. Stepanyants, "Automated tracing of neurites from light microscopy stacks of images.," *Neuroinformatics*, vol. 9, no. 2-3, pp. 263–78, Sept. 2011.

[7] S. K. Schmitz, J. J. Hjorth, R. M. S. Joemai, R. Wijntjes, S. Eijgenraam, P. de Bruijn, C. Georgiou, A. P. H. de Jong, A. van Ooyen, M. Verhage, L. N. Cornelisse, R. F. Toonen, W. J. H. Veldkamp, and W. Veldkamp, "Automated analysis of neuronal morphology, synapse number and synaptic recruitment.," *Journal of neuroscience methods*, vol. 195, no. 2, pp. 185–93, Feb. 2011.

[8] X. Bai, E. Hancock, and R. C. Wilson, "Geometric characterization and clustering of graphs using heat kernel embeddings," *Image and Vision Computing*, vol. 28, no. 6, pp. 1003 – 1021, 2010.

[9] M. Belkin and P. Niyogi, "Laplacian eigenmaps for dimensionality reduction and data representation," *Neural Computation*, vol. 15, no. 6, pp. 1373–1396, 2003.

[10] F. Meyer, "Topographic distance and watershed lines," *Signal Processing*, vol. 38, no. 1, pp. 113 – 125, 1994.

[11] K. E. Mardia and P. E. Jupp, *Directional Statistics*, Wiley, 2000.

[12] Ulrike von Luxburg, "A tutorial on spectral clustering," *Statistics and Computing*, vol. 17, no. 4, pp. 395–416, Dec. 2007.